AGU PUBLICATIONS

Geophysical Research Letters

RESEARCH LETTER
10.1002/2017GL073270

Key Points:
- Newly developed HALO in situ measurements give insight in stratospheric trace gas distributions in the lower Antarctic vortex
- A high amount of activated chlorine reservoir species and redistributed nitric acid in the lower Antarctic polar stratosphere was observed
- Upper vortex air was transported to the flight altitude of HALO at 12 to 14 km

Supporting Information:
- Supporting Information S1

Correspondence to:
T. Jurkat,
tina.jurkat@dlr.de

Citation:
Jurkat, T., et al. (2017), Depletion of ozone and reservoir species of chlorine and nitrogen oxide in the lower Antarctic polar vortex measured from aircraft, *Geophys. Res. Lett.*, *44*, 6440–6449, doi:10.1002/2017GL073270.

Received 16 MAR 2017
Accepted 14 MAY 2017
Accepted article online 22 MAY 2017
Published online 28 JUN 2017

Depletion of ozone and reservoir species of chlorine and nitrogen oxide in the lower Antarctic polar vortex measured from aircraft

T. Jurkat[1], C. Voigt[1,2], S. Kaufmann[1], J.-U. Grooß[3], H. Ziereis[1], A. Dörnbrack[1], P. Hoor[2], H. Bozem[2], A. Engel[4], H. Bönisch[4,5], T. Keber[4], T. Hüneke[6], K. Pfeilsticker[6], A. Zahn[5], K. A. Walker[7], C. D. Boone[8], P. F. Bernath[9], and H. Schlager[1]

[1]Deutsches Zentrum für Luft- und Raumfahrt, Institut für Physik der Atmosphäre, Oberpfaffenhofen, Germany, [2]Institute for Atmospheric Physics, Johannes Gutenberg Universität Mainz, Mainz, Germany, [3]Forschungszentrum Jülich, Institut für Energie- und Klimaforschung: Stratosphäre, Jülich, Germany, [4]Institute for Atmospheric and Environmental Sciences, Goethe Universität Frankfurt, Frankfurt, Germany, [5]Karlsruhe Institute of Technology, Karlsruhe, Germany, [6]Institute of Environmental Physics, Universität Heidelberg, Heidelberg, Germany, [7]Department of Physics, University of Toronto, Toronto, Ontario, Canada, [8]Department of Chemistry, University of Waterloo, Waterloo, Ontario, Canada, [9]Department of Chemistry and Biochemistry, Old Dominion University, Norfolk, Virginia, USA

Abstract Novel airborne in situ measurements of inorganic chlorine, nitrogen oxide species, and ozone were performed inside the lower Antarctic polar vortex and at its edge in September 2012. We focus on one flight during the Transport and Composition of the LMS/Earth System Model Validation (TACTS/ESMVal) campaign with the German research aircraft HALO (High-Altitude LOng range research aircraft), reaching latitudes of 65°S and potential temperatures up to 405 K. Using the early winter correlations of reactive trace gases with N_2O from the Atmospheric Chemistry Experiment-Fourier Transform Spectrometer (ACE-FTS), we find high depletion of chlorine reservoir gases up to ~40% (0.8 ppbv) at 12 km to 14 km altitude in the vortex and 0.4 ppbv at the edge in subsided stratospheric air with mean ages up to 4.5 years. We observe denitrification of up to 4 ppbv, while ozone was depleted by 1.2 ppmv at potential temperatures as low as 380 K. The advanced instrumentation aboard HALO enables high-resolution measurements with implications for the oxidation capacity of the lowermost stratosphere.

Plain Language Summary Chemistry climate models reveal large uncertainties in the future ozone projection until the end of the century in the lower polar and midlatitude stratosphere. One process that impacts the ozone lifetime during the polar winter is the formation of active chlorine from chlorine reservoir species. Here we present high-resolution measurements performed aboard the new German research aircraft HALO (High-Altitude LOng range research aircraft) in the lower Antarctic vortex in winter 2012. We find significant amounts of active chlorine in the lower vortex that has been transported from higher altitudes and latitudes to the flight altitude of HALO (~14 km). This enhanced activated chlorine content has implications on the ozone lifetime in this region. Our measurements complement satellite observations but feature higher-altitude resolution and extend to lower altitudes. With our case study we investigate the intersection of midlatitude and polar air as well as the effects of transport from the upper to the lower polar vortex. These process studies help to improve chemistry climate models.

1. Introduction

The strongest ozone loss in the stratosphere occurs in Austral spring over Antarctica. Heterogeneous reactions on polar stratospheric clouds (PSCs) and cold binary aerosols that form in the cold winter polar stratosphere [*Crutzen and Arnold*, 1986; *Drdla and Müller*, 2012] trigger the conversion of reservoir species into ozone-depleting chlorine and bromine compounds [*Solomon et al.*, 1986]. The return of sunlight in Antarctic spring allows photolytic ozone destroying cycles to occur. Hydrogen chloride (HCl) and chlorine nitrate ($ClONO_2$) are the most important reservoir gases, which dominate the stratospheric chlorine budget in unperturbed conditions at the beginning of the winter. Sedimentation of nitric acid (HNO_3) containing PSC particles causes a loss of reactive nitrogen at the PSC formation altitude (denitrification). The lack of nitrogen oxides reduces deactivation of active chlorine (reformation of chlorine reservoir species like $ClONO_2$) and enhances

ozone destruction [*Fahey et al.*, 1990]. Here we refer to active chlorine as the sum of ClO, $2xCl_2O_2$, Cl, HOCl, and $2xCl_2$.

Transport and mixing of extravortex air may also alter the composition of the Antarctic vortex [*Parrondo et al.*, 2014]. Both lead to ozone, chlorine reservoir, and nitric acid-rich filaments, masking chemical activation and destruction, in particular, at the vortex edge. The transport across and chemical composition in the vicinity of the vortex edge play an important role in the persistence of the chemical ozone loss since both, a weaker mixing and the state of chemical processing, may delay ozone recovery in the vortex during spring [*Roscoe et al.*, 2012; *Newman et al.*, 2004].

Chemistry climate model simulations projecting the time scale of the ozone hole recovery are particularly sensitive to the present and future amount of inorganic chlorine ($Cl_y \approx HCl + ClONO_2 + ClO_x$ with $ClO_x \approx ClO + 2xClOOCl$) [*Eyring et al.*, 2007, 2013], and therefore, accurate measurements and process studies on chlorine species modifying stratospheric ozone are needed. Particularly, future projections of ozone changes in the southern polar and extratropical lowermost stratosphere (LMS) are highly uncertain [*Bekki et al.*, 2013]. Activated chlorine, depleted ozone, and nitric acid redistribution have been derived using tracer-tracer correlations measured from satellite, aircraft, and balloons of chemically active species with long-lived tracers [e.g., *Fahey et al.*, 1990; *Wilmouth et al.*, 2006; *Müller et al.*, 2005]. Due to the challenging accessability of the Antarctic LMS, the number of observations from aircraft is limited, yet they provide a better spatial resolution and accuracies of a multitude of tracer measurements compared to satellite observations at aircraft cruise altitudes and below. Almost one and a half decades after the last airborne stratospheric measurements over Antarctica [e.g., *Carli et al.*, 2000], we present a new generation of measurements to investigate the effects of a changing climate and related lower stratospheric temperatures on the composition of the lower Antarctic vortex. Here we show a case study on a set of new airborne measurements obtained for one flight on 13 September 2012 in the lower Antarctic polar vortex and its edge with the German research aircraft HALO (High-Altitude and LOng Range research aircraft) during the TACTS/ESMVal (Transport and Composition of the LMS/Earth System Model Validation) mission. We first describe the trace gas measurements aboard HALO with particular focus on the new simultaneous measurements of chlorine reservoir species. The measurements are supported by data from the European Centre for Medium-Range Weather Forecasts (ECMWF). Further, we explain the tracer-tracer correlation method and discuss chlorine activation, nitric acid redistribution, and ozone depletion in the lower polar vortex and the implications for the LMS. Uncertainties of the method are discussed in the supporting information. This work is a pilot study for upcoming airborne HALO missions in the polar LMS.

2. Instrumentation Aboard HALO

2.1. Airborne Chemical Ionization Mass Spectrometer AIMS

AIMS is a recently designed chemical ionization mass spectrometer, operated with an electrical discharge source and in-flight calibration [*Jurkat et al.*, 2016]. Measurements of HCl, HNO_3, SO_2, and nitrous acid (HONO) in the midlatitude tropopause are described in *Voigt et al.* [2014] and *Jurkat et al.* [2014]. Alternatively, AIMS can be operated in the water vapor mode [*Kaufmann et al.*, 2016; *Voigt et al.*, 2016]. In addition to the HNO_3 and HCl measurements, we now show simultaneous, highly spatially resolved $ClONO_2$ measurements performed by AIMS in the lower Antarctic stratosphere at potential temperatures between 300 and 405 K. SF_5^- ions are used as reagent ions to selectively detect $ClONO_2$ via fluoride transfer [*Marcy et al.*, 2005]. A detailed discussion of the measurement sensitivity and accuracy is given in the supporting information. The accuracies of HCl and HNO_3 are 12% and 16% [*Jurkat et al.*, 2016], respectively. The estimated accuracy for $ClONO_2$ is expected to be 20% (upper limit), which is about a factor of 2 to 3 better than the accuracy of satellite-retrieved $ClONO_2$ concentrations at this altitude (see supporting information). Except for polar regions, $ClONO_2$ was below the 1σ detection limit of 15 pptv with a 1.3 s time resolution (and less than 5 pptv at 30 s averages). The measurements benefit from high spatial resolution (~220 m) and high precision (10%), complementing and validating remote sensing instruments [*Ungermann et al.*, 2015]. In particular, AIMS represents an independent in situ technique of simultaneous measurements of $ClONO_2$ and HCl that supports established airborne instruments using resonance fluorescence or tunable diode laser techniques [*Webster et al.*, 1994; *Wilmouth et al.*, 2006]. In comparison to earlier measurement techniques (e.g., Aircraft laser infrared absorption spectrometer [*Webster et al.*, 1994]), the higher time resolution (1.3 s versus 30 s) of AIMS combined with a similar detection limit (15 pptv versus tens of pptv), along with its simultaneous measurements of relevant stratospheric tracers (HCl and HNO_3), make AIMS unique relative to previously deployed instruments on high-flying aircraft.

2.2. Other In Situ and Remote Sensing Instruments on HALO

Onboard N_2O measurements are based on the three-channel tunable diode laser instrument for atmospheric research (TRIHOP) used during SPURenstofftransport in der Tropopausenregion (trace gas transport in the tropopause region), SPURT [*Hoor et al.*, 2004]. With a new quantum cascade laser setup, N_2O data achieved a 2σ precision of 1.1 ppbv and a stability of the instrument of 2.2 ppbv at a time resolution of 0.1 Hz before applying the postflight data correction [*Müller et al.*, 2016].

O_3 mixing ratios were measured using a combination of a chemiluminescence sensor and a UV photometer named FAIRO at a rate of 10 Hz with high precision and reproducibility of 0.5% and 1.5% [*Zahn et al.*, 2012].

Nitrogen oxide (NO) was measured by AENEAS (Atmospheric nitrogen oxides measuring system). AENEAS is a two-channel chemiluminescence detector in connection with a gold converter. One channel is used for reduction of higher oxidation stages of reactive nitrogen oxides ($NO_y = NO_2 + HNO_3 + HONO + PAN, \ldots$) to NO [*Ziereis et al.*, 2000]. The detection limit for NO is 8 pptv (2σ) with an overall accuracy of 8% at 0.5 ppbv at 1 Hz time resolution. In the stratosphere, approximately 90% of NO_y is in the form of HNO_3 [*Neuman et al.*, 2002]. A comparison of the sum of $ClONO_2$ and HNO_3 from AIMS and NO_y from AENEAS yields an agreement within 6% inside the polar vortex [*Jurkat et al.*, 2016]. Comparison of data from the limb sounding Michelson Interferometer GLORIA [*Ungermann et al.*, 2015] confirms the robustness of the AIMS HNO_3 measurements. Due to the good agreement of the HALO instruments and the comparability of the HNO_3 measurements by Atmospheric Chemistry Experiment-Fourier Transform Spectrometer (ACE-FTS), we limit our analysis to HNO_3 instead of the generally used NO_y.

The sum of estimated inorganic chlorine Cl_y is calculated from correlations of CFC-12 with other halogenated source gases, which were derived from balloon-borne cryogenic whole air sampling inside the Arctic polar vortex [see, e.g., *Engel et al.*, 2006; *Wetzel et al.*, 2015]. The correlations have then been corrected to account for changing tropospheric trends based on the method of *Plumb et al.* [1999], as explained in *Wetzel et al.* [2015] and applied to GhOST (Gas chromatograph for the Observation of Stratospheric Tracers) measurements of CFC-12. The GhOST instrument is a multichannel gas chromatograph with a precision of 0.5% for CFC-12 and 1% for SF_6 during the TACTS/ESMVal campaign, thus providing precise and fast measurements of CFC-12 and SF_6 with a time resolution of 0.1 Hz. Mean age of air is inferred from SF_6 measurements with an overall precision of 0.3 years and an estimated accuracy of 0.6 years, as explained in *Engel et al.* [2006]. The uncertainty of the inferred Cl_y is on the order of 0.1–0.2 ppbv.

The mini-Differential Optical Absorption Spectroscopy (DOAS) instrument is a limb sensor to detect a suite of UV/visible absorbing species in atmospheric daylight using the Differential Optical Absorption Spectroscopy (DOAS) technique [*Platt and Stutz*, 2008]. Measurements of NO_2 mixing ratios at flight altitude are retrieved using radiative transfer modeling [*Deutschmann et al.*, 2011] in combination with a novel scaling technique [*Werner et al.*, 2017]. The detection limit for NO_2 is about 10 pptv [*Hüneke et al.*, 2017]. The accuracy is about 10 pptv for low NO_2 and $\pm$ 15% for higher NO_2, whatever is greater.

3. ACE-FTS Measurements

The Atmospheric Chemistry Experiment (ACE) is a satellite mission on board the Canadian satellite SCISAT-1, measuring a set of more than 30 trace gases, such as $ClONO_2$, HCl, HNO_3, O_3, and N_2O by means of Fourier transform spectrometry [*Bernath et al.*, 2005]. ACE-FTS has been used in the past decade to derive stratospheric trace gas concentrations for polar research [*Santee et al.*, 2008; *WMO*, 2014]. Within this study, ACE-FTS data have been employed to derive the early winter reference correlations of the investigated reactive trace gases and N_2O, assuming unperturbed stratospheric conditions during this time period. For the data version 2.2, the uncertainty for N_2O is 15% (5–30 km) [*Strong et al.*, 2008] and for HCl is 5% to 10% (20–50 km) [*Mahieu et al.*, 2008]. For $ClONO_2$ and HNO_3 data version 3.5 [*Boone et al.*, 2005, 2013] was used. The uncertainties for $ClONO_2$ and HNO_3 are 29% to 6% (17–38 km) and below 5% (20–40 km) [*Sheese et al.*, 2015, 2016], respectively. The region and time period chosen to derive these early winter tracer correlations as well as the accuracy of the measurements at lower altitudes is specified in the supporting information.

4. Synoptic Situation and Air Mass History

The TACTS/ESMVal mission comprised 13 flights from latitudes of 68°N to 65°S and 25°E to 74°W with more than 120 flight hours. The aim of the campaign was to study the transport and composition of the UT/LMS

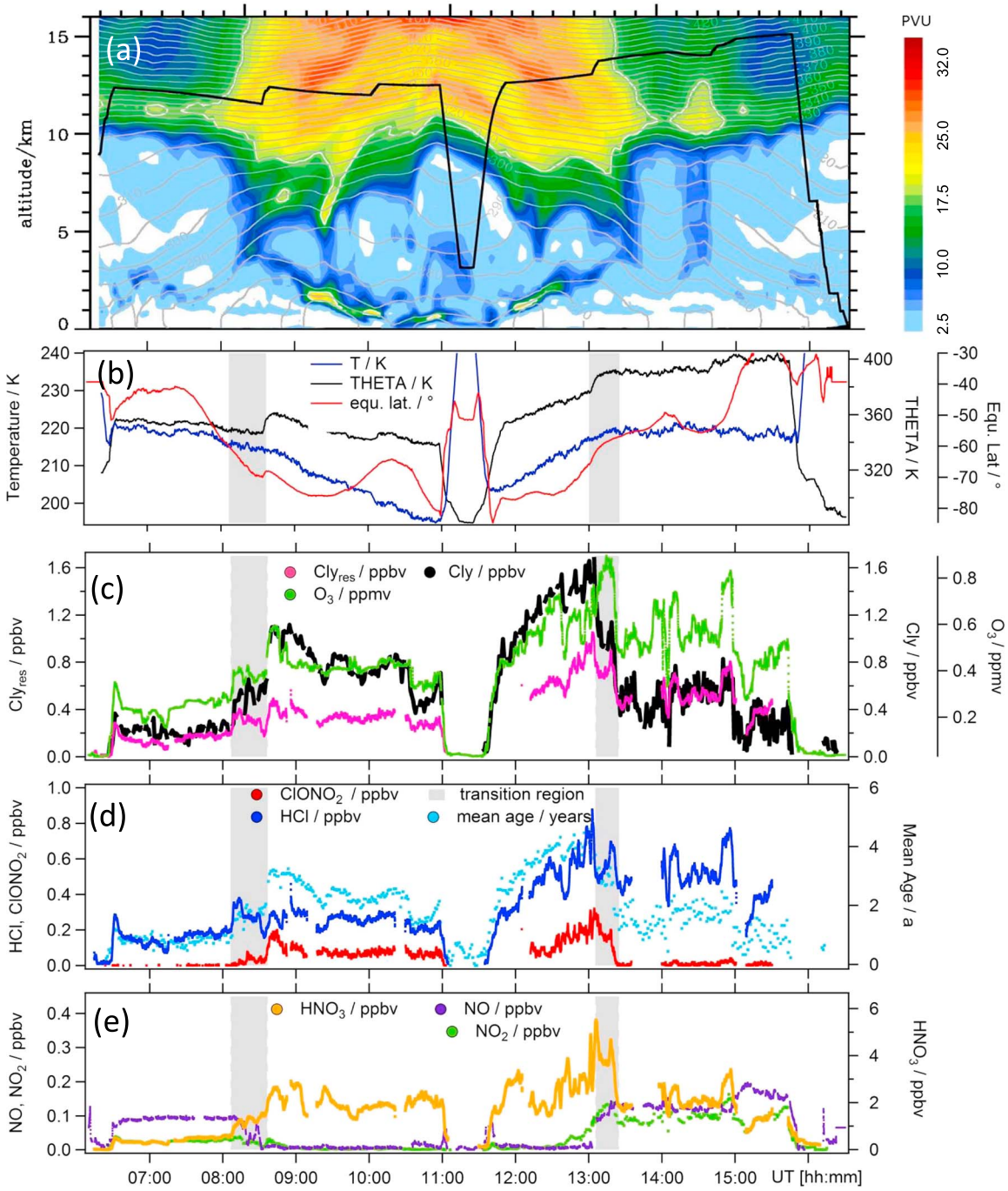

Figure 1. (a) A curtain plot of the MPV along the flight track on 13 September 2012 is shown. The GPS altitude of HALO is given in black. The white contour shows the 17 MPVU isoline; isentropes are shown in gray. The aircraft enters the vortex around 8:00 UT at an altitude of 12 km and performs a stepwise ascent up to 14.3 km and a dive at 11:00 UT. (b) The temperature and potential temperature measured aboard HALO and the calculated equivalent latitude along the flight track. (c–e) Time lines of trace gas measurements on 13 September 2012. Shown are the chlorine reservoir species $Cl_{y,res}$(=$ClONO_2$+HCl), inferred Cl_y, and O_3 (Figure 1c); HCl, $ClONO_2$, and mean age (Figure 1d); and the nitrogen oxide containing species HNO_3, NO, and NO_2 (Figure 1e). The gray bars show the transition region between vortex and extravortex air.

region and provide observations for global climate model validation [*Eyring et al.*, 2007]. A demonstration of the aircraft's capability to fly long distance and high altitude was given during a flight on 13 September 2012 heading toward the Antarctic continent. With takeoff and landing in Cape Town the aircraft reached 65°S, with a measurement time of approximately 5 h within the vortex boundaries. The dynamical situation encountered during the flight is shown in Figures 1a and 1b by ECMWF operational analysis interpolated in space and time on the HALO flight track. The vortex, represented by enhanced modified potential vorticity

(MPV, color coded) [*Lait*, 1994] with its dynamical edge indicated by the white 17 MPVU isoline [*Müller and Günther*, 2003], extended far north and was first crossed at 47°S. Additionally, given in Figure 1a is the GPS altitude of HALO. The flight altitude was mainly between 11.5 km and 14.3 km inside the vortex and 14.9 km outside, except during a dive down to 3 km altitude (Figure 1a). Inside the vortex, the aircraft crossed isentropes between 320 K and 385 K and equivalent latitudes of 60°S to 85°S (Figure 1b). Except for the short period between 10:30 UT and 11:00 UT, temperatures were above 200 K (Figure 1b), thus too high to have caused heterogeneous reactions on particle surfaces. Trajectory calculations (see supporting information Figure S2 and [*Rolf et al.*, 2015]) show that the air mass encountered between 12 UT and 13 UT experienced a 30 hPa pressure increase with an associated warming of up to 20 K within the last 2 days; thus, air from high altitudes and latitudes with temperatures below the PSC formation temperature was sampled inside the vortex. At the time of the measurement the polar vortex was well established and ozone depletion had already generated an ozone hole of 18 million km^2 in size [*Strahan et al.*, 2014]. The 2012 ozone hole in Antarctica was the second smallest in the last 20 years and reached its maximum on 22 September 2012 (ESRL, NOAA). Thus, the conditions encountered may be representative for polar stratospheric conditions with declining ozone hole areas.

5. Trace Gas Measurements on 13 September 2012

Figures 1c–1e give an overview of the trace gas measurements during the flight on 13 September 2012. Shown is the time series of the trace gas combination of the chlorine reservoir species HCl+$ClONO_2$ (hereafter called $Cl_{y,res}$), Cl_y, and O_3 (c); HCl, $ClONO_2$, and mean age (d); and the nitrogen oxide containing species HNO_3, NO, and NO_2 (e). In general, we find midlatitude stratospheric air, vortex air, and a mixture of both. The transition region between vortex and extravortex air south of the dynamical edge is marked by the gray shaded area and was inferred using the method of *Greenblatt et al.* [2002]. The lower boundary of the vortex (17 MPVU isoline) is crossed two more times vertically at 11 UT and 11:45 UT during the dive.

5.1. Extravortex Trace Gas Measurements

Focusing on midlatitude stratospheric tracers (HCl, HNO_3, and O_3) which were sampled at the beginning and end of the flight, we find similar features in the time series with a compact linear correlation [*Jurkat et al.*, 2014], presented in section 6. NO_2 and NO (NO_x) are at expected stratospheric levels [*Neuman et al.*, 2002], corresponding to rather young stratospheric air with a mean age of air below 2 years. Here the sum of HCl and $ClONO_2$ agrees with the inferred Cl_y, underlining the confidence in the trace gas measurements. The good agreement also suggests the absence of significant amounts of other active chlorine compounds.

5.2. Vortex Trace Gas Measurements

Inside the vortex, the well-correlated relationships of stratospheric tracers break up while NO_x remains at the detection limit. The small-scale variability in $ClONO_2$ encountered between 12 and 13 UT can be found similarly in HCl and HNO_3 largely following the MPV pattern at HALO flight altitude of 13 km. Here N_2O reaches its lowest value of 217 ppbv which corresponds to a mean age of 4.5 years, suggesting descended, aged air from higher altitudes. Ozone reaches a maximum of 0.7 ppmv at 12:35 UT. The ratios of O_3 and Cl_y and the ratio of $Cl_{y,res}$ and Cl_y are significantly decreased in the vortex compared to the extravortex ratios, suggesting ozone depletion and chlorine activation in this region. A quantitative analysis is presented in section 6.

5.3. Transition Between Vortex and Extravortex Air

The transition region is governed by transport and mixing of young midlatitude and aged vortex air. This region is characterized by a steep gradient of NO_x concentrations from some 0.1 ppbv in the lower midlatitude stratosphere to concentrations near the detection limit (~10 pptv) in the polar vortex, as well as a gradient in the mean age and inferred Cl_y. The transition region is crossed at ~350 K and a second time at ~385 K by the aircraft and spans a range of 409 km in the lower part and narrows to 250 km at the upper level (assuming a flight track perpendicular to the vortex edge). In the transition region, we observe a maximum of 0.29 ppbv $ClONO_2$ and 0.87 ppbv O_3 together with midlatitude stratospheric NO_x in close vicinity. The difference between Cl_y and $Cl_{y,res}$ decreases from 0.4 ppbv (equivalent to about 40% activated chlorine) at 13:07 UT at the most southern part of the transition region to 0 ppbv at the dynamical vortex edge in the north. Thus, using the high-resolution aircraft measurements, we find that depletion of reservoir species is even prevalent in the transition region, unresolvable to satellite measurements. The distinct and homogenous trace gas relationships inside the vortex and in the midlatitude stratosphere, however, suggest an efficient transport barrier between the two regions at the time of the measurements.

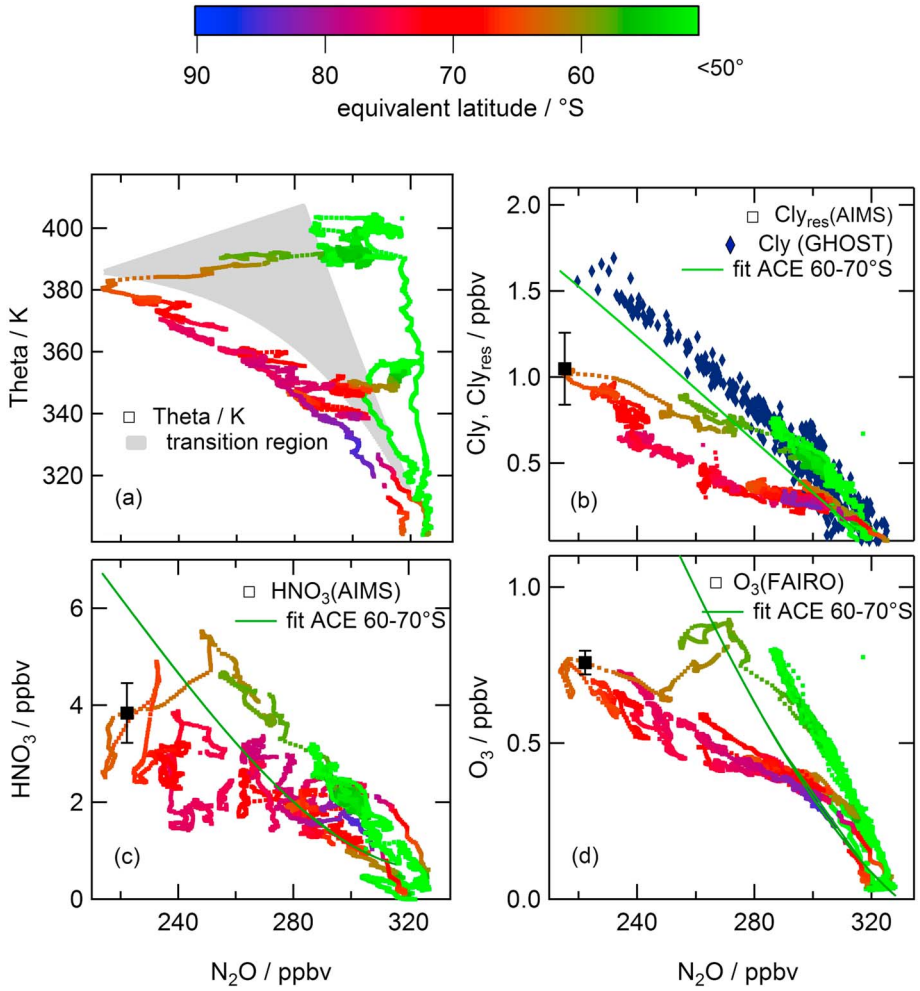

Figure 2. (a) The potential temperature profile of N_2O for the airborne data from 13 September color coded with the equivalent latitude. The gray shaded area represents the transition region. Further, (b) tracer-tracer correlations of Cl_y and N_2O (marine diamonds), $Cl_{y,res}$(= HCl+ $ClONO_2$), and N_2O; (c) HNO_3 and N_2O; and (d) O_3 and N_2O are shown. The 60°S–70°S-equivalent latitude fit of the early winter reference from ACE-FTS is given for each correlation. The black squares with example error bars show the uncertainties of a single point measurement.

6. Method: Early and Late Winter Tracer-Tracer Correlation

The depletion of chlorine reservoir species in the vortex is assessed using the difference of satellite retrieved and in situ measured trace gas correlations. We compare the correlation of N_2O with $Cl_{y,res}$ from ACE-FTS at the beginning of the winter with the correlation of N_2O with Cl_y inferred from in situ measurements of CFC-12 on 13 September 2012. Similarly for nitric acid redistribution and ozone depletion, the correlation of in situ measured HNO_3 and N_2O as well as O_3 and N_2O is compared to the corresponding early winter satellite measurements. A direct comparison of airborne and satellite measurements was not possible since the satellite measurement was at ~80°S, thus not in the measurement range of the aircraft.

Figures 2a and 2b show the correlation of potential temperature and N_2O as well as $Cl_{y,res}$ and N_2O measured aboard HALO. Error bars (representing an example of the accuracy of the measurements) are given for single measurement points. The color code represents the calculated equivalent latitude for each data point. The polar branch with equivalent latitudes >65°S is clearly separated from the midlatitude branch with equivalent latitudes <50°S, intercepting at 290 ppbv N_2O. The transition region inferred after *Greenblatt et al.* [2002] is marked in gray. Mixing between midlatitude and processed vortex air is observed twice in the $Cl_{y,res}$-N_2O correlation inside the transition region: One mixing line below 350 K and one at 385 K suggests quasi-isentropic mixing at the transition region.

To derive the activated fraction of inorganic chlorine reservoir gases, the correlation of Cl_y inferred from in situ measurements and N_2O is shown in marine diamonds (Figure 2a). At the midlatitude, extravortex branch, HCl (and $ClONO_2$), makes up most of the inorganic chlorine, in line with observations of *Wilmouth et al.* [2006], stating that most of the activation takes place inside the vortex boundaries. The polar branch of the HNO_3-N_2O correlation shown in Figure 2c is noisier and less compact since it may be additionally affected by redistribution of HNO_3. The ozone measurements (Figure 2d) show a similar behavior as the chlorine reservoir species with two separate branches and mixing lines.

The fits of the ACE-FTS retrievals for the trace gas correlations of $Cl_{y,res}$, HNO_3 and O_3 versus N_2O derived from measurements at the beginning of the polar winter are also shown in Figures 2b–2d. Third-order polynomials were fitted to the ACE-FTS $Cl_{y,res}$, HNO_3, and O_3 to N_2O correlations (see supporting information Figure S3 and Table S1). For clarity, only the fit for equivalent latitudes between 60°S and 70°S is shown. The choice of the equivalent latitude bin for the fit changes the result by less than 10%; thus, the correlation is very robust. Inside the vortex, in situ measurements inferred Cl_y and the fit from ACE-FTS data differ by about 0.2 ppbv; potential reasons and an assessment of the uncertainties of the method are discussed in the supporting information.

7. Chlorine Activation and Nitric Acid Redistribution in the Vortex

Figure 3a shows the difference ($\Delta Cl_{y,res}$) of in situ measured $Cl_{y,res}$ and Cl_y inferred from in situ measurements (marine diamonds) (here called "GhOST-AIMS") as a function of potential temperature inside the vortex between 340 K and 382 K. Additionally, $\Delta Cl_{y,res}$ derived with the fit of ACE from equivalent latitudes between 60°S and 70°S and in situ measured $Cl_{y,res}$ (here called "ACE-AIMS") is shown in Figure 3a. Negative $\Delta Cl_{y,res}$ represents the amount of depleted chlorine reservoir species, thus activated chlorine from inorganic species. Figures 3b and 3c show the difference (ΔHNO_3 and ΔO_3) in measured and derived nitric acid and ozone from the fitted ACE-FTS measurements for equivalent latitudes between 60°S and 70°S as a function of potential temperature in the vortex. The average 2K bins for almost two completed profiles are shown in red. Negative ΔHNO_3 and ΔO_3 suggest nitric acid removal due to PSC particle sedimentation and ozone depletion, respectively. Regions near 0 (marked with a gray vertical line) and above are related to unperturbed conditions.

Layers of denitrification up to 4 ppbv were mainly encountered above 360 K accompanied by dehydration at these low altitudes [*Rolf et al.*, 2015]. The relationship between dehydration and denitrification (not shown) largely follows the pattern described in *Fahey et al.* [1990], typical for Antarctic conditions at potential temperatures around 425 K, implying the existence of ice PSCs over the course of the air mass history that sediment and transport condensed water and nitric acid to lower altitudes. The relationship of water vapor and nitric acid, and thus its information on PSC formation, has been preserved during the recent adiabatic air mass descent. $\Delta HNO_3 > 0$ potentially related to nitrification was mainly measured between 340 K and 360 K, in line with Arctic measurements [*Dibb et al.*, 2006].

Compared to ΔHNO_3, $\Delta Cl_{y,res}$ and ΔO_3 are more homogenously distributed with a maximum at 370 K of 0.8 ppbv and 1.1 ppmv, respectively, for the in situ measurements. These mixing ratios correspond to a chlorine reservoir depletion of 40% and ozone depletion of 60%. Lowest $\Delta Cl_{y,res}$ and ΔO_3 coincide with denitrified regions. Both indicate the existence of HNO_3-containing PSC particles that activated chlorine and led to ozone depletion with subsequent removal of HNO_3 by sedimentation of the particles. As a consequence of low HNO_3 concentrations, chlorine deactivation was decelerated and ozone depletion ongoing. To assess the chlorine partitioning between the two reservoir gases, the ratio of $ClONO_2$ and HCl and the ratio of NO_x and HNO_3 are shown in Figure 3d. $ClONO_2$/HCl ranges between 0 and 0.4; thus, HCl is always more abundant than $ClONO_2$. The ratio of $ClONO_2$/HCl is enhanced in layers where the ratio of NO_x/HNO_3 is elevated over the generally low background of 0.01. Thus, we assume that the availability of NO_x has started to change the chlorine partitioning from HCl to $ClONO_2$ where enhanced NO_x was present, e.g., at the 360 K and 375 K isentropes.

Similar measurements of $ClONO_2$, HCl, ClO, and OClO have been performed aboard the ER-2 during winter and spring 2000 in the Arctic polar vortex [*Grooß et al.*, 2002; *Wilmouth et al.*, 2006] above 400 K potential temperature. Our observation of 40% depleted chlorine reservoir gases extends the region where active chlorine can be found, which until now has only been observed by Arctic airborne measurements at temperatures below 200 K [*Wilmouth et al.*, 2006]. Since activation and uptake on particles is restricted to temperatures below 195 K, here vortex conditions with active chlorine seem to have been preserved during the recent adiabatic transport from higher altitudes and lower temperatures supported by trajectory calculations (Figure 2S).

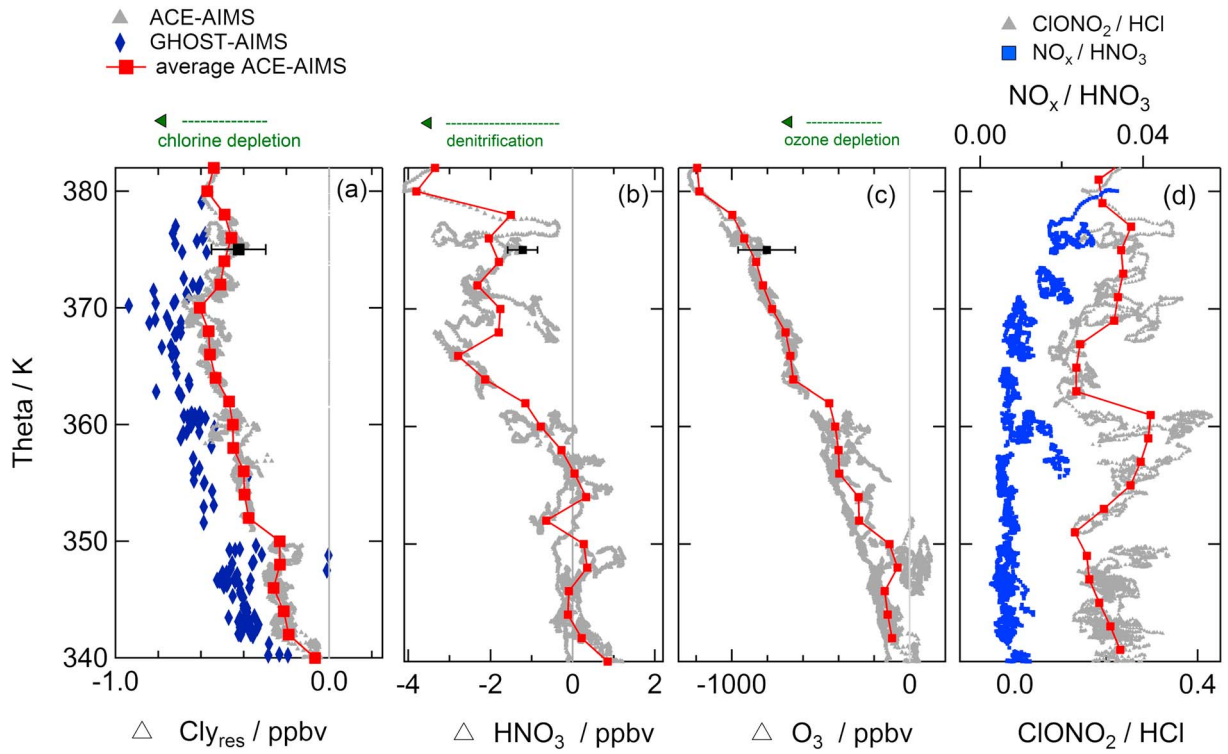

Figure 3. (a) Depleted inorganic chlorine reservoir gases ($\Delta Cl_{y,res}$), (b) redistributed nitric acid (ΔHNO_3), and (c) depleted ozone (ΔO_3) derived with the early vortex reference from ACE-FTS and in situ measurements from AIMS and TRIHOP (here called "ACE-AIMS") as a function of potential temperature for in-vortex measurements. Gray dots represent the measured 1 Hz data, while red squares represent the 2K potential temperature averages. The gray vertical line is the 0 mark. $\Delta Cl_{y,res}$ derived with in situ measurements of $Cl_{y,res}$ and inferred Cl_y are represented by marine diamonds (here called "GHOST-AIMS"). (d) The ratio of $ClONO_2$/HCl (gray) together with the ratio NO_x/HNO_3 (blue) as a function of potential temperature is shown. The black squares with example error bars (Figures 3a–3c) show the uncertainty of the derived depleted concentrations of $Cl_{y,res}$, HNO_3 and O_3.

8. Summary and Implications

We present a new measurement technique for detection of low concentrations of the chlorine reservoir species $ClONO_2$ and HCl in the UTLS. In the Antarctic polar LMS during one flight in winter 2012, inorganic chlorine reservoir gases that were depleted up to 0.8 ppbv have been inferred using the combination of airborne and satellite measurements. Simultaneously, nitric acid redistribution and ozone depletion have been derived by comparison of tracer-tracer correlations at the beginning of the polar winter with the measurements on 13 September 2012. The method benefits from the good temporal and spatial coverage of the satellite measurements in the middle stratosphere and the accurate, high-resolution airborne measurements in the LMS. We suggest that vortex conditions between 340 K and 382 K potential temperature as encountered by HALO around 145 hPa have been preserved during the adiabatic air mass descent that started 2 days before the measurement. Our measurements at relatively high temperatures at the lower vortex and its edge extend the region where activated chlorine was observed previously [*Wilmouth et al.*, 2006; *Santee et al.*, 2008].

If observed more frequently, the availability of active chlorine near the tropopause may have implications for the ozone and methane lifetime in this region where small changes of these climate relevant species modify the long-wave radiation budget and thus have a large impact on the surface temperature [*Riese et al.*, 2012]. In this altitude and latitude range, the methane loss rates are highest for the chemical reaction with Cl [*Stenke et al.*, 2012] due to the lack of OH. The frequency and impact of transported active chlorine to the northern latitude LMS, however, remains to be explored with a higher number of aircraft observations.

The trend of midlatitude ozone changes since the year 2000 derived from models, ground-based, and satellite measurements shows the largest variability in the tropopause region [*WMO*, 2014], still lacking a full attribution of processes leading to these changes. Locally activated chlorine on, e.g., cirrus clouds [*Solomon et al.*, 1997] or chlorine radicals from other sources [*Baker et al.*, 2016] are generally low in concentration and cannot exceed the enhanced amount of transported active chlorine found in the lower polar vortex at 12 to 14 km

by HALO. Thus, transport of active chlorine from higher altitudes together with chlorine and bromine released from the degradation of very short lived halogenated species are important but yet unquantified causes for ozone depletion in the polar and subpolar LMS [*Hossaini et al.*, 2015] particularly in the periphery of the ozone hole [*Fernandez et al.*, 2017]. This study can be used for comparison to model simulations and recent, extensive HALO measurements in the lower Arctic stratosphere during the cold winter 2015/2016. Our measurements complement satellite retrievals but feature higher spatial resolution and extend to lower altitudes, permitting investigation of the intersection of midlatitude and polar air as well as the effects of transport from the upper to the lower polar vortex.

Acknowledgments
This research was funded by the Deutsche Forschungsgemeinschaft (DFG, HALO-SPP 1294) via grants JU 3059/1-1 and VO 1504/4-1 (T.J. and C.V.), PF-384/7-1, PF-384/7-2, and PF384/9-1 (K.P. and T.H.). C.V., T.J., and S.K. thank financing by the Helmholtz Association under contract W2/W3-60. We also thank three anonymous reviewers for their valuable comments. The Atmospheric Chemistry Experiment (ACE), also known as SCISAT, is a Canadian-led mission mainly supported by the Canadian Space Agency and the Natural Sciences and Engineering Research Council of Canada. The in situ data can be found in the HALO database (https://halo-db.pa.op.dlr.de/). The ACE-FTS data can be downloaded from http://www.ace.uwaterloo.ca. (registration required).

References

Baker, A. K., C. Sauvage, U. R. Thorenz, P. van Velthoven, D. E. Oram, A. Zahn, C. A. M. Brenninkmeijer, and J. Williams (2016), Evidence for strong, widespread chlorine radical chemistry associated with pollution outflow from continental Asia, *Nat. Sci. Rep.*, *6*, 36821.

Bekki, S., A. Rap, V. Poulain, S. Dhomse, M. Marchand, F. Lefevre, P. Forster, S. Szopa, and M. Chipperfield (2013), Climate impact of stratospheric ozone recovery, *Geophys. Res. Lett.*, *40*, 2796–2800, doi:10.1002/grl.50358.

Bernath, P. F., et al. (2005), Atmospheric chemistry experiment (ACE): Mission overview, *Geophys. Res. Lett.*, *32*, L15S01, doi:10.1029/2005GL022386.

Boone, C. D., R. Nassar, K. A. Walker, Y. Rochon, S. D. McLeod, C. P. Rinsland, and P. F. Bernath (2005), Retrievals for the atmospheric chemistry experiment Fourier-transform spectrometer, *Appl. Opt.*, *44*(33), 7218–7231, doi:10.1364/AO.44.007218.

Boone, C. D., K. A. Walker, and P. F. Bernath (2013), Version 3 retrievals for the Atmospheric Chemistry Experiment Fourier Transform Spectrometer (ACE-FTS), in *The Atmospheric Chemistry Experiment ACE at 10: A Solar Occultation Anthology*, edited by P. Bernath, pp. 103–127, A. Deepak, Hampton, Va.

Carli, B., U. Cortesi, C. E. Blom, M. P. Chipperfield, G. De Rossi, and G. Redaelli (2000), Airborne Polar Experiment Geophysica Aircraft in Antarctica (APE-GAIA), *SPARC Newsl.*, *15*, 21–24.

Crutzen, P. J., and F. Arnold (1986), Nitric acid cloud formation in the cold Antarctic stratosphere: A major cause for the springtime ozone hole, *Nature*, *324*(6098), 651–655.

Deutschmann, T., et al. (2011), The Monte Carlo atmospheric radiative transfer model McArtim: Introduction and validation of Jacobians and 3D features, *J. Quant. Spectrosc. Radiat. Transfer*, *112*(6), 1119–1137, doi:10.1016/j.jqsrt.2010.12.009.

Dibb, J. E., E. Scheuer, M. Avery, J. Plant, and G. Sachse (2006), In situ evidence for renitrification in the Arctic lower stratosphere during the polar aura validation experiment (PAVE), *Geophys. Res. Lett.*, *33*, L12815, doi:10.1029/2006GL026243.

Drdla, K., and R. Müller (2012), Temperature thresholds for chlorine activation and ozone loss in the polar stratosphere, *Ann. Geophys.*, *30*(7), 1055–1073, doi:10.5194/angeo-30-1055-2012.

Engel, A., et al. (2006), Observation of mesospheric air inside the arctic stratospheric polar vortex in early 2003, *Atmos. Chem. Phys.*, *6*(1), 267–282, doi:10.5194/acp-6-267-2006.

Eyring, V., et al. (2007), Multimodel projections of stratospheric ozone in the 21st century, *J. Geophys. Res.*, *112*, D16303, doi:10.1029/2006JD008332.

Eyring, V., et al. (2013), Long-term ozone changes and associated climate impacts in CMIP5 simulations, *J. Geophys. Res. Atmos.*, *118*, 5029–5060, doi:10.1002/jgrd.50316.

Fahey, D. W., K. K. Kelly, S. R. Kawa, A. F. Tuck, M. Loewenstein, K. R. Chan, and L. E. Heidt (1990), Observations of denitrification and dehydration in the winter polar stratospheres, *Nature*, *344*(6264), 321–324.

Fernandez, R. P., D. E. Kinnison, J.-F. Lamarque, S. Tilmes, and A. Saiz-Lopez (2017), Impact of biogenic very short-lived bromine on the Antarctic ozone hole during the 21st century, *Atmos. Chem. Phys.*, *17*(3), 1673–1688, doi:10.5194/acp-17-1673-2017.

Greenblatt, J. B., et al. (2002), Defining the polar vortex edge from an N_2O: Potential temperature correlation, *J. Geophys. Res.*, *107*(D20), 8268, doi:10.1029/2001JD000575.

Grooß, J.-U., et al. (2002), Simulation of ozone depletion in spring 2000 with the Chemical Lagrangian Model of the Stratosphere (CLaMS), *J. Geophys. Res.*, *107*(D20), 8295, doi:10.1029/2001JD000456.

Hoor, P., C. Gurk, D. Brunner, M. I. Hegglin, H. Wernli, and H. Fischer (2004), Seasonality and extent of extratropical TST derived from in-situ CO measurements during SPURT, *Atmos. Chem. Phys.*, *4*(5), 1427–1442, doi:10.5194/acp-4-1427-2004.

Hossaini, R., M. P. Chipperfield, S. A. Montzka, A. Rap, S. Dhomse, and W. Feng (2015), Efficiency of short-lived halogens at influencing climate through depletion of stratospheric ozone, *Nat. Geosci.*, *8*(3), 186–190.

Hüneke, T., et al. (2017), The novel halo mini-DOAS instrument: Inferring trace gas concentrations from air-borne UV/visible limb spectroscopy under all skies using the scaling method, *Atmos. Meas. Tech. Discuss.*, *2017*, 1–42, doi:10.5194/amt-2017-89.

Jurkat, T., et al. (2014), A quantitative analysis of stratospheric HCl, HNO_3, and O_3 in the tropopause region near the subtropical jet, *Geophys. Res. Lett.*, *41*, 3315–3321, doi:10.1002/2013GL059159.

Jurkat, T., S. Kaufmann, C. Voigt, D. Schäuble, P. Jeßberger, and H. Ziereis (2016), The airborne mass spectrometer AIMS—Part 2: Measurements of trace gases with stratospheric or tropospheric origin in the UTLS, *Atmos. Meas. Tech.*, *9*(4), 1907–1923, doi:10.5194/amt-9-1907-2016.

Kaufmann, S., C. Voigt, T. Jurkat, T. Thornberry, D. W. Fahey, R.-S. Gao, R. Schlage, D. Schäuble, and M. Zöger (2016), The airborne mass spectrometer AIMS—Part 1: AIMS-H2O for UTLS water vapor measurements, *Atmos. Meas. Tech.*, *9*(3), 939–953.

Lait, L. R. (1994), An alternative form for potential vorticity, *J. Atmos. Sci.*, *51*(12), 1754–1759, doi:10.1175/1520-0469.

Mahieu, E., et al. (2008), Validation of ACE-FTS v2.2 measurements of HCl, HF, CCl_3F and CCl_2F_2 using space-, balloon- and ground-based instrument observations, *Atmos. Chem. Phys.*, *8*(20), 6199–6221, doi:10.5194/acp-8-6199-2008.

Marcy, T., R. Gao, M. Northway, P. Popp, H. Stark, and D. Fahey (2005), Using chemical ionization mass spectrometry for detection of HNO_3, HCl, and $ClONO_2$ in the atmosphere, *Int. J. Mass Spectrom.*, *243*(1), 63–70, doi:10.1016/j.ijms.2004.11.012.

Müller, R., and G. Günther (2003), A generalized form of Lait's modified potential vorticity, *J. Atmos. Sci.*, *60*(17), 2229–2237, doi:10.1175/1520-0469(2003).

Müller, R., S. Tilmes, P. Konopka, J.-U. Grooß, and H.-J. Jost (2005), Impact of mixing and chemical change on ozone-tracer relations in the polar vortex, *Atmos. Chem. Phys.*, *5*(11), 3139–3151, doi:10.5194/acp-5-3139-2005.

Müller, S., et al. (2016), Impact of the Asian monsoon on the extratropical lower stratosphere: Trace gas observations during TACTS over Europe 2012, *Atmos. Chem. Phys.*, *16*(16), 10,573–10,589, doi:10.5194/acp-16-10573-2016.

Neuman, J. A., et al. (2002), Fast-response airborne in situ measurements of HNO_3 during the Texas 2000 Air Quality Study, *J. Geophys. Res.*, *107*(D20), 4436, doi:10.1029/2001JD001437.
Newman, P. A., S. R. Kawa, and E. R. Nash (2004), On the size of the Antarctic ozone hole, *Geophys. Res. Lett.*, *31*, L21104, doi:10.1029/2004GL020596.
Parrondo, M. C., M. Gil, M. Yela, B. J. Johnson, and H. A. Ochoa (2014), Antarctic ozone variability inside the polar vortex estimated from balloon measurements, *Atmos. Chem. Phys.*, *14*(1), 217–229, doi:10.5194/acp-14-217-2014.
Platt, U., and J. Stutz (2008), *Differential Optical Absorption Spectroscopy (DOAS), Principle and Applications*, Springer, Heidelberg.
Plumb, I. C., P. F. Vohralik, and K. R. Ryan (1999), Normalization of correlations for atmospheric species with chemical loss, *J. Geophys. Res.*, *104*(D9), 11,723–11,732, doi:10.1029/1999JD900014.
Riese, M., F. Ploeger, A. Rap, B. Vogel, P. Konopka, M. Dameris, and P. Forster (2012), Impact of uncertainties in atmospheric mixing on simulated UTLS composition and related radiative effects, *J. Geophys. Res.*, *117*, D16305, doi:10.1029/2012JD017751.
Rolf, C., et al. (2015), Transport of Antarctic stratospheric strongly dehydrated air into the troposphere observed during the HALO-ESMVal campaign 2012, *Atmos. Chem. Phys.*, *15*(16), 9143–9158, doi:10.5194/acp-15-9143-2015.
Roscoe, H. K., W. Feng, M. P. Chipperfield, M. Trainic, and E. F. Shuckburgh (2012), The existence of the edge region of the Antarctic stratospheric vortex, *J. Geophys. Res.*, *117*, D04301, doi:10.1029/2011JD015940.
Santee, M. L., I. A. MacKenzie, G. L. Manney, M. P. Chipperfield, P. F. Bernath, K. A. Walker, C. D. Boone, L. Froidevaux, N. J. Livesey, and J. W. Waters (2008), A study of stratospheric chlorine partitioning based on new satellite measurements and modeling, *J. Geophys. Res.*, *113*, D12307, doi:10.1029/2007JD009057.
Sheese, P. E., C. D. Boone, and K. A. Walker (2015), Detecting physically unrealistic outliers in ACE-FTS atmospheric measurements, *Atmos. Meas. Tech.*, *8*(2), 741–750, doi:10.5194/amt-8-741-2015.
Sheese, P. E., et al. (2016), Validation of ACE-FTS version 3.5 NO_y species profiles using correlative satellite measurements, *Atmos. Meas. Tech.*, *9*(12), 5781–5810, doi:10.5194/amt-9-5781-2016.
Solomon, S., R. R. Garcia, F. S. Rowland, and D. J. Wuebbles (1986), On the depletion of Antarctic ozone, *Nature*, *321*(6072), 755–758.
Solomon, S., S. Borrmann, R. R. Garcia, R. Portmann, L. Thomason, L. R. Poole, D. Winker, and M. P. McCormick (1997), Heterogeneous chlorine chemistry in the tropopause region, *J. Geophys. Res.*, *102*(D17), 21,411–21,429, doi:10.1029/97JD01525.
Stenke, A., R. Deckert, and K.-D. Gottschaldt (2012), *Methane Modeling: From Process Modeling to Global Climate Models*, chap. 47, pp. 781–797, Springer, Berlin, doi:10.1007/978-3-642-30183-4_9.
Strahan, S. E., A. R. Douglass, P. A. Newman, and S. D. Steenrod (2014), Inorganic chlorine variability in the Antarctic vortex and implications for ozone recovery, *J. Geophys. Res. Atmos.*, *119*, 14,098–14,109, doi:10.1002/2014JD022295.
Strong, K., et al. (2008), Validation of ACE-FTS N_2O measurements, *Atmos. Chem. Phys.*, *8*(16), 4759–4786, doi:10.5194/acp-8-4759-2008.
Ungermann, J., et al. (2015), Level 2 processing for the imaging Fourier transform spectrometer GLORIA: Derivation and validation of temperature and trace gas volume mixing ratios from calibrated dynamics mode spectra, *Atmos. Meas. Tech.*, *8*(6), 2473–2489, doi:10.5194/amt-8-2473-2015.
Voigt, C., P. Jeßberger, T. Jurkat, S. Kaufmann, R. Baumann, H. Schlager, N. Bobrowski, G. Giuffrida, and G. Salerno (2014), Evolution of CO_2, SO_2, HCl, and HNO_3 in the volcanic plumes from Etna, *Geophys. Res. Lett.*, *41*, 2196–2203, doi:10.1002/2013GL058974.
Voigt, C., et al. (2016), ML-CIRRUS—The airborne experiment on natural cirrus and contrail cirrus with the high-altitude long-range research aircraft HALO, *Bull. Am. Meteorol. Soc.*, *98*, 271–288, doi:10.1175/BAMS-D-15-00213.1.
Webster, C. R., R. D. May, C. A. Trimble, R. G. Chave, and J. Kendall (1994), Aircraft (ER-2) laser infrared absorption spectrometer (ALIAS) for in-situ stratospheric measurements of HCl, N_2O, CH_4, NO_2, and HNO_3, *Appl. Opt.*, *33*(3), 454–472, doi:10.1364/AO.33.000454.
Werner, B., et al. (2017), Probing the subtropical lowermost stratosphere and the tropical upper troposphere and tropopause layer for inorganic bromine, *Atmos. Chem. Phys.*, *17*(2), 1161–1186, doi:10.5194/acp-17-1161-2017.
Wetzel, G., et al. (2015), Partitioning and budget of inorganic and organic chlorine species observed by MIPAS-B and TELIS in the Arctic in March 2011, *Atmos. Chem. Phys.*, *15*(14), 8065–8076, doi:10.5194/acp-15-8065-2015.
Wilmouth, D. M., R. M. Stimpfle, J. G. Anderson, J. W. Elkins, D. F. Hurst, R. J. Salawitch, and L. R. Lait (2006), Evolution of inorganic chlorine partitioning in the Arctic polar vortex, *J. Geophys. Res.*, *111*, D16308, doi:10.1029/2005JD006951.
WMO (2014), Scientific Assessment of Ozone Depletion: 2014, *Global Ozone Res. and Monit. Project Rep. No. 55*, 145 pp., Geneva, Switzerland.
Zahn, A., J. Weppner, H. Widmann, K. Schlote-Holubek, B. Burger, T. Kühner, and H. Franke (2012), A fast and precise chemiluminescence ozone detector for eddy flux and airborne application, *Atmos. Meas. Tech.*, *5*(2), 363–375, doi:10.5194/amt-5-363-2012.
Ziereis, H., H. Schlager, P. Schulte, P. F. J. van Velthoven, and F. Slemr (2000), Distributions of NO, NO_x, and NO_y in the upper troposphere and lower stratosphere between 28° and 61°N during POLINAT 2, *J. Geophys. Res.*, *105*(D3), 3653–3664, doi:10.1029/1999JD900870.